Composite Structures 160 (2017) 964–975

Contents lists available at ScienceDirect

Composite Structures

journal homepage: www.elsevier.com/locate/compstruct

Exploring how optimal composite design is influenced by model fidelity and multiple objectives

Shreyas Joglekar, Kayla Von Hagel, Mark Pankow, Scott Ferguson *

Department of Mechanical and Aerospace Engineering, North Carolina State University, Raleigh, NC 27695, USA

ARTICLE INFO

Article history:
Received 6 January 2016
Revised 19 October 2016
Accepted 21 October 2016
Available online 22 October 2016

Keywords:
Composite panel design
Multi-objective optimization
Finite element model
Analytic model
Solution seeding

ABSTRACT

This paper explores how optimal configuration of a composite panel is influenced by the choice of analysis model – analytic or computational – and the consideration of multiple objectives. While past research has explored aspects of this problem separately – composite ply orientation, multiple load scenarios, and multiple performance objectives – there has been limited work addressing the interactions between these factors. Three loading scenarios are considered in this work, and it is demonstrated that for certain scenarios an analytical model likely over-predicts composite performance. Further, for complex loading scenarios it is impossible to develop an analytical model. However, this work also demonstrates that the use of analytical models can be advantageous. Analytical models can provide similar estimates to computational models for some loading cases at significantly reduced computational expense. More importantly, it is also shown how solutions from the analytical model, which can be relatively cheap to find computationally, can be used to seed the initial designs of a Finite Element-based optimization. Run time reductions as large as 80% are demonstrated when these informed seeded designs are used, even when the designs were created for a different set of loading scenarios.

1. Introduction

Composite laminate design problems often involve large design spaces that are discrete or mixed-integer. Engineers control the number of layers and tailor the stacking sequence and fiber orientation to the load path of a structure [1–3]. Additionally, choices have to be made between (1) incorporating time-saving, low-fidelity models or (2) accepting the computational cost and/or risk of missing a deadline by using high-fidelity models. After the problem is formulated and the analysis model is chosen, an optimization is completed and the solutions are used to guide composite design decisions [4–8].

Early researchers formulated single objective optimization problems with reduced design spaces and used analytical models to diminish computational cost. Improved computational resources have led to a greater prevalence of computational models that are more complex and the consideration of larger design spaces that require advanced optimization techniques. The presence of multiple loading scenarios further complicates the selection of an optimal configuration. An optimal composite layup for a single loading scenario is likely to be drastically sub-optimal across multiple loading scenarios. The need to navigate such trade-offs is common, especially in aerospace engineering applications where composites may experience uniaxial tension and transverse compression, uniaxial tension and biaxial compression, and load cases with out-of-plane pressure.

Yet little, if any, research exists that explores problems with multiple load scenarios and competing performance objectives. In light of more complete theoretical [9–11] and computational models [2,12] that have been created from increased understanding of composite panel design, a better understanding of the relationship between model selection, computational cost, and quality of solution is needed.

The objective of this paper is to explore the differences in optimal composite configuration when a choice is made between using an analytical model or a computational Finite Element (FE) model in the presence of multiple performance objectives across three different loading conditions. The research presented in this paper compares where analytical and computational models exhibit similar and different solution behavior. This outcome is important because it directly addresses the challenge of when each model can be used to facilitate exploration (generating new design candidates and analyzing them cheaply) versus where exploitation may

* Corresponding author.
E-mail addresses: ssjoglek@ncsu.edu (S. Joglekar), kavonhag@ncsu.edu (K. Von Hagel), mrpankow@ncsu.edu (M. Pankow), scott_ferguson@ncsu.edu (S. Ferguson).

http://dx.doi.org/10.1016/j.compstruct.2016.10.089
0263-8223/

be needed using more computationally expensive models to ensure the estimated performance of a design is accurate.

Previous research has considered multiple objectives for a single load case when continuous angle orientations are used [13–15]. Conversely, computational cost is managed in research that considers multiple load cases by restricting the number of possible orientation angles (typically to 5 or less) and relying on single objective formulations [16]. This paper extends existing efforts by allowing each ply to take on one of 19 possible fiber orientations and by formulating multi-objective problem formulations for each of the three loading scenarios considered. Outcomes from each model are then analyzed for differences in terms of estimated system performance and the design configurations that comprise the final solution sets. Computational expense is also considered, and opportunities for leveraging a combination of analytical and computational models are discussed.

The layout of this paper is as follows: Section 2 provides relevant background information regarding how FE methods (analytical and computational) and optimization approaches (problem formulation, algorithm development) have been applied to composite panel design problems. The research approach and problem formulations are introduced in Section 3, and results are presented in Section 4. These results are discussed in Section 5 while conclusions and avenues for future work are presented in Section 6.

2. Brief discussion of theoretical foundations

Advancements made in modeling composite panels and optimizing are presented in this section. The goal is not to comprehensively cover all possible research associated with the analysis of composite panels, or different approaches taken toward optimizing them. Rather, prior work advancing the state-of-the-art is highlighted and current limitations are discussed.

2.1. Modeling of composite materials

Early composite analysis used Classical Laminated Plate Theory (CLPT) which was an analytical formulation [9–11]. CLPT enabled researchers to explore simple laminates where only a single ply layer was optimized [10,11]. Other researchers extended the work to predict buckling loads and first ply failure [9]; however, only simple structures (plates or shells) could be considered and the inclusion of multi-angle structures of complex geometry was not permitted. Therefore, researchers naturally expanded into Finite Element analysis, which is capable of predicting the response for much more complicated loading scenarios.

Initial FE models were implemented using in-house codes. For example, initial optimization using these codes centered on plates subjected to transverse pressure and optimized with respect to the mass and deflection [8]. Since then, numerous commercial FE codes have been investigated with different failure theories. Shell elements are often used as the basis of the analysis as they are more computationally efficient than 3D solid elements and are well suited for thin laminate analysis. Plate buckling with first ply failure optimization was performed using the commercial FE code SAMCEF with Hashin failure criteria [13]. Almeida and Awruch consider multiple load case scenarios [16], but the choice of fiber orientation in these analyses was limited to no more than 5 orientation angles. Lee et al. extended the feasible set of fiber orientation angles to 12; however, only a single load case was considered [14].

Computational resource improvements have facilitated the transition from analytical methods of analysis to FE-based computational methods, enabling more complex problems to be explored. Yet, even the computational power offered by a typical desktop computer can result in run times on the order of 15–30 min per simulation. For thousands of iteration calls this can result in a large computational expense. Additionally, optimization algorithms have seen significant advancements in the form of gradient estimation, the creation of new heuristic approaches, and parallelization associated with population-based strategies. Overall, these advancements improve solution quality while simultaneously reducing computational expense, as discussed in the next section.

2.2. Optimization of composite materials

The choice of algorithm used to optimize a composite material often depends on the structure of the problem formulation – discrete or continuous variables, constraints, number of objectives – and the availability of computational resources needed to solve the problem in a timely manner. Techniques used in the literature include direct search techniques [3], gradient-based approaches [3,4], applications of heuristics and greedy behavior [3,12,5,6,17], hybridizations of existing methods [3,18,19], and tailored algorithms that make specific use of composite properties [7,20,21]. Direct search methods eliminate the computational cost associated with calculating the derivative [22], but such approaches are generally applied to problem formulations that contain only a few design variables due to decreased convergence rates [3]. For example, partitioning methods were used in [23] because only a single variable problem was considered. Small design spaces also allow for enumeration strategies [24,25], where the outcomes of the enumeration can be used to guide design space down-selection [26] and to identify which variables have the greatest impact on performance measures [27].

Gradient-based methods offer faster convergence than direct and heuristic methods, but often lack the ability to escape local minimum and require continuous variables for gradient calculation [28] which limit applicability toward composite panel optimization. The limitations of gradient-based approaches for more complex problem formulations, and those with multiple minima, have led to increased application of heuristic and greedy algorithms [3,29]. For example, Irisarri et al. used an Evolutionary Algorithm to maximize the buckling and collapse loads of a composite stiffened panel [13]. The stacking sequences of the skin and stiffeners were determined while maintaining a constant panel mass. Genetic algorithms have also seen increased use when considering objectives such as strength, buckling loads, weight, and stiffness [3] because of their zero-order nature, the ability to tailor algorithm performance, and their ability to find global minimums in multimodal spaces.

The consideration of multiple objectives when formulating the problem requires the use of different classes of optimization algorithms. Early efforts used fiber orientation and a weighted sum approach to maximize prebuckling stiffness, initial postbuckling stiffness and the critical buckling load of uniaxially loaded laminated plates [10]. Walker et al. used a golden section method to determine the Pareto optimal value of fiber angle when maximizing the buckling loads associated with torsional and axial buckling [11]. Genetic algorithms and finite element models have been combined in [8] to simultaneously minimize mass and the deflection of laminated composite structures, and a Pareto-based evolutionary algorithm has been used when minimizing the number of plies while maximizing buckling margins [9].

A challenge of multiobjective problem formulations is that the design space associated with them tends to be quite large. Computational efficiency becomes a significant consideration, and inadequate tuning of heuristic algorithms that lead to poor overall solution quality may further increase computational expense. While analytic models for composite panel design problems may not be as accurate as Finite Element models, the design space is

less computationally expensive to explore when they are used. A missing contribution is identifying how the advantages offered by an analytic model can be leveraged. An approach to answering this question is introduced in the next section.

3. Research approach

While the application of optimization strategies to composite panel design is not new, previous work has placed serious restrictions on the number of layers that could be considered, the orientation angles that could be used, the number and complexity of objective functions, and whether the problem formulation could include constraints. The study in this paper removes, or relaxes, some of these restrictions by allowing the orientation angle of each ply in an 8-layer composite to be chosen from a set of 19 angle orientations. The optimization problem formulation also includes two competing objective functions and three different load cases are considered. Further, as the computational cost of an optimization is strongly influenced by the expense associated with each objective function evaluation, two different evaluation methods are considered. Solutions to these different formulations are explored for similarities to understand how model fidelity can be leveraged to achieve computational savings or where it leads to different predictions of performance that must be further analyzed.

The problem investigated in this work is a pressurized fuselage skin modeled as a two-dimensional plate. The material in this analysis is a square (20-inch by 20-inch) graphite epoxy composite with a constant thickness of 0.01 in. and simply supported edges. Pressure on the panel induces loads in the axial and hoop directions. Additionally, a compressive load may exist, accounting for fuselage bending. Associated material properties are listed in Table 1. The loading scenarios considered are: (1) uniaxial tension and transverse compression, (2) uniaxial tension and non-uniform biaxial compression, and (3) uniaxial tension and non-uniform biaxial compression with out-of-plane pressure. Load scenarios are depicted in Fig. 1. In all three cases, buckling failure is examined for compressive loads. In load scenarios (2) and (3), the compressive load in the direction of tension is 10% of the compressive load in the transverse direction.

A computational model based on FE allows for complex structures to be considered under a wide variety of loading scenarios. Analytic methods have higher computational efficiency, but accuracy decreases as composite complexity increases. Further, different formulations of the analytic model are needed for different loading scenarios. To explore how the choice of analysis model and load scenario influences the optimal results, the approach in Fig. 2 was developed. For Load Scenarios 1 and 2, non-dominated points associated with a multiobjective optimization problem are identified using both a Finite Element and analytic model. These non-dominated points are then cross-evaluated to better understand how model choice influences predicted composite performance. Non-dominated solutions obtained from the analytic model for Load Scenarios 1 and 2 are then cross-evaluated to explore how changes to load scenario might cause previously optimal designs to underperform. An analytic model form is not possible for Load Scenario 3. For this loading case, the focus is on understanding how using previously identified optimal solutions to a different loading scenario (here the non-dominated solutions associated with the analytic model for Load Scenario 2) can be used to reduce computational expense. This is achieved by using these non-dominated solutions as an initial starting point for the optimization of the composite in Load Scenario 3.

Table 1
Material properties: constituent properties of composite.

Material properties	Values
E_1	30×10^6 psi
E_2	0.75×10^6 psi
ν_{12}	0.25
G_{12}	0.375×10^6 psi
X_t	150×10^3 psi
Y_t	6×10^3 psi
S	10×10^3
X_c	100×10^3 psi
Y_c	17×10^3 psi

3.1. Selecting an analytical and computational model

Critical loads are calculated by considering the loading scenario and the analysis model being used. For the analytic models, critical tensile loads are calculated assuming CLPT and analytic expressions for Hashin's failure criteria [30]:

1. Fiber failure in tension: $F_f^t = \left(\frac{\sigma_{11}}{X_t}\right)^2 + \left(\frac{\tau_{12}}{S}\right)^2$.
2. Fiber failure in compression: $F_f^c = \left(\frac{\sigma_{11}}{X_c}\right)^2$
3. Matrix failure in tension: $F_m^t = \left(\frac{\sigma_{22}}{Y_t}\right)^2 + \left(\frac{\tau_{12}}{S}\right)^2$
4. Matrix failure in compression: $F_m^c = \left(\frac{\sigma_{22}}{2S}\right)^2 + \left(\frac{\tau_{12}}{S}\right)^2 + \left[\left(\frac{Y_c}{2S}\right)^2 - 1\right] * \frac{\sigma_{22}}{Y_c}$

σ_{11}, σ_{22}, and τ_{12} indicate stress in the fiber direction, stress in the transverse direction and shear stress for individual lamina, respectively. For uniaxial tensile loading, only one component out of stress and moment resultant is non-zero. Using Eq. (1), failure strains for each laminate are calculated. Since Hashin's criteria is a unidirectional failure criteria, the laminate strains are transformed into each individual ply direction and the smallest critical load value is selected to indicate first ply failure.

$$\begin{bmatrix} N \\ M \end{bmatrix} = \begin{bmatrix} A & B \\ B & D \end{bmatrix} \begin{bmatrix} \varepsilon \\ \kappa \end{bmatrix} \tag{1}$$

Plate edges are assumed to be free. An exact solution for critical buckling load is not available and most available solutions assume the bending-extension matrix to be zero. A solution which considers a non-zero B matrix exists for anti-symmetric angle ply laminates ($\pm\theta_n$) and is used in this analysis to calculate critical buckling loads. However, the terms A_{16}, A_{26}, B_{11}, B_{12}, B_{22}, B_{66}, D_{16} and D_{26} are still assumed to be zero. Eq. (2) [31] is used to calculate the critical buckling load N_0. Table 2 gives the variable descriptions for Eq. (2).

$$\begin{aligned} N_0 = \frac{\pi^2}{R^2 b^2 (m^2 + kn^2R^2)} \Big\{ & D_{11}m^4 + 2m^2n^2R^2(D_{12} + 2D_{66}) \\ & + D_{22}n^4R^4 - \frac{1}{J_1}[mJ_2(B_{16}m^2 + 3B_{26}n^2R^2) \\ & + nRJ_3(3B_{16}m^2 + B_{26}n^2R^2)] \Big\} \end{aligned} \tag{2}$$

where

$$J_1 = (A_{11}m^2 + A_{66}n^2R^2)(A_{66}m^2 + A_{22}n^2R^2) - (A_{12} + A_{66})^2 m^2n^2R^2$$

$$\begin{aligned} J_2 = {} & (A_{11}m^2 + A_{66}n^2R^2)(B_{16}m^2 + 3B_{26}n^2R^2) \\ & - (A_{12} + A_{66})n^2R^2(3B_{16}m^2 + 3B_{26}n^2R^2) \end{aligned}$$

$$\begin{aligned} J_3 = {} & (A_{66}m^2 + A_{22}n^2R^2)(3B_{16}m^2 + B_{26}n^2R^2) \\ & - (A_{12} + A_{66})n^2R^2(B_{16}m^2 + 3B_{26}n^2R^2) \end{aligned}$$

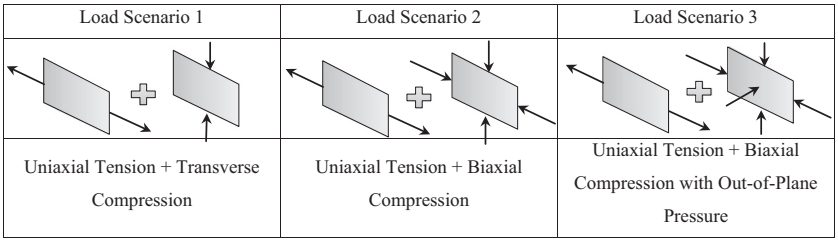

Fig. 1. Load scenarios: description of load cases in this analysis.

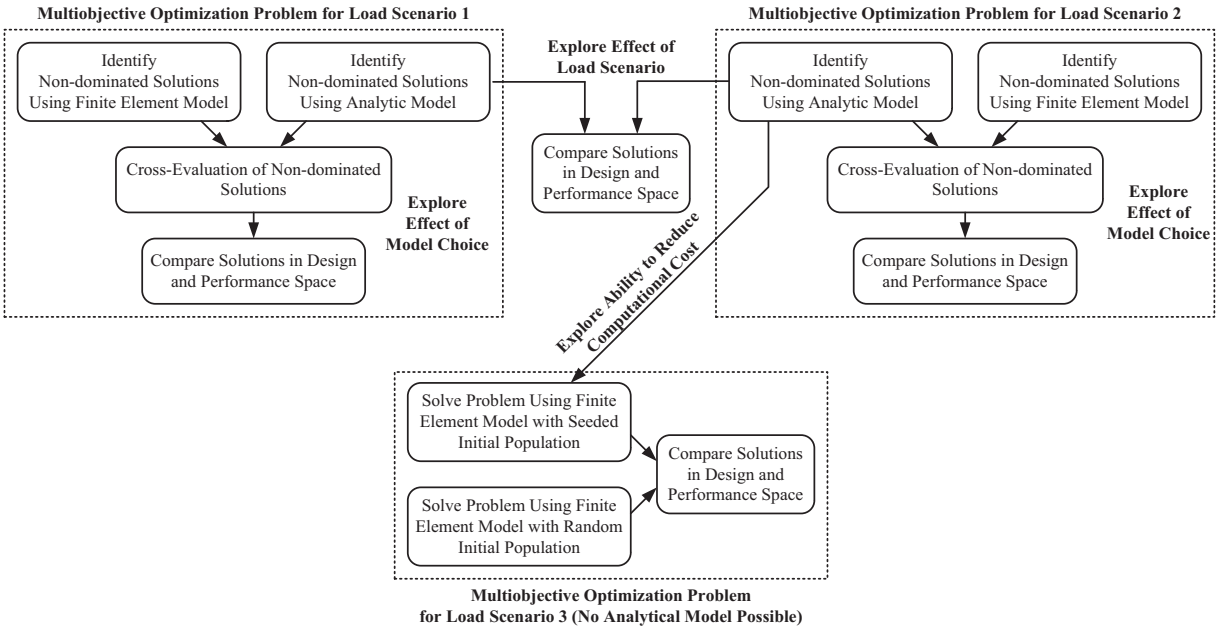

Fig. 2. Research approach: a pathway toward solution exploration.

Table 2
Analytic solution variables: terms within Eq. (2).

Variable	Description
b	Plate length
$R = \frac{a}{b}$	Plate aspect ratio
m	Buckling mode shape parameter in length
n	Buckling mode shape parameter in width
k	Biaxial loading parameter (for uniaxial loads, $k = 0$ and for uniform biaxial loads, $k = 1$)

For plate buckling, the lowest buckling load does not typically occur for $m = 1$ and $n = 1$ [32]. Thus the critical buckling load is calculated for different combinations of m and n. Further, analytical solutions take only a fraction of the time required for FE analysis.

The problem can be treated as one of plane stress for the FE model, as the dimension of the plate in the thickness direction is less than 1% of the in-plane dimensions. Load calculations and stress analysis were carried out using commercial software, ABAQUS [30]. Since random ply laminates can have large values in the associated bending-extending (B) matrix, this matrix cannot be neglected. To model the system, 400 quadrilateral elements with 8 nodes and reduced integration are used. Progressive damage of the laminate under applied tension is checked by Hashin's failure criteria [13]. The tensile load is applied in small increments until the value of any of the Hashin failure criteria in any ply reaches 1. For compressive loads, buckling analysis is carried out to determine the critical load resultant. All edges are assumed to be simply supported.

3.2. Formulate and solve the optimization problems

Each composite is comprised of 8 plies. Fiber angle orientation is constrained by a lower bound of −90 degrees, an upper bound of 90 degrees, and can take on values in increments of 10 degrees. Typical manufacturing constraints of symmetry and balance are not considered, though direct enforcement is a topic of future work. For each load scenario, two objective functions were considered where the loads are maximized. Mathematically, the optimization problem is formulated as Eq. (3).

$$\begin{aligned} &\text{Maximize :} \quad \lambda_1(\boldsymbol{X}),\ \lambda_2(\boldsymbol{X}) \\ &\text{Subject to :} \quad \forall x \in \boldsymbol{X} = \{\boldsymbol{x_1}, \boldsymbol{x_2}, \ldots, \boldsymbol{x_8}\}, \quad -90 \leqslant x \leqslant 90 \\ &x_i \quad mod \quad 10 = 0 \end{aligned} \tag{3}$$

In this equation, λ_i is an objective function and represents the loading conditions that is being maximized. These objectives are a function of the design string X, representing the vector of orientation angles for each ply. x_i is the orientation angle of each layer.

The multi-objective optimization problem is solved using a Multi-Objective Genetic Algorithm (MOGA) based on NSGA-II [33]. This algorithm was chosen because of the multimodal nature of the problem, the discrete nature of the design variables, and the high cost of obtaining gradient information [3,29]. The initial population consisted of 80 design strings randomly created using the

available set of fiber orientation angles. Eighty percent of the population was crossed over using arithmetical crossover with a mixing value of 0.4.

The mutation rate was fixed at 5%, and mutated designs were created by randomly adding or subtracting 10 degrees to a single ply. Parallel processing was implemented to reduce run time [34,35]. To determine convergence, the hyper-volume of the Pareto frontier was used. If three generations were completed in which the hyper-volume did not change, the MOGA terminated.

3.3. Comparison of solutions

The final step of the approach is to compare the results produced by the computational FE and analytic models. Two major comparisons are considered in this work. Solutions are compared across model type to identify (1) if the Pareto optimal solutions from the computational FE and analytic model exist in the same region of the performance space, and (2) if similar trades in estimated composite performance can be characterized by specific fiber orientations in the various plies.

Such a study is necessary to determine if using different models and load cases produce designs that are fundamentally similar from a design configuration perspective. If configuration differences are found, understanding the nature of these differences will provide insight into the design decisions (and tradeoffs) that must be made when designing a composite panel. This paper seeks to compare the optimal fiber orientation angles within each composite design across both the computational FE and analytic method and the different load scenarios.

4. Results

It was expected that the results of each optimization would show analytic solutions to be less accurate because of simplifications and assumptions associated with model development. However, an advantage of these models is that they took approximately 4% the computational run-time required to converge than the optimization processes using the FE model. Since the objectives defined in the problem formulation are to maximize the critical loads, better solutions are found as the solution approaches the upper right corner of each plot. The following subsections align with the research approach described in Fig. 2.

4.1. Load Case 1: uniaxial tension and transverse buckling

The non-dominated Pareto solutions are displayed in Fig. 3 for the objectives of uniaxial tension and transverse buckling. When focus of the algorithm is on a single objective, such as in the Top and Bottom Regions that represent the endpoints of the Pareto frontiers, both models predict similar performances. However, away from these endpoints the solutions from the analytic model withstand larger buckling loads at a given tension than the solutions obtained from the computational FE model.

In general, past research has shown that CLPT solutions tend to over-predict critical buckling loads [36]. This can be partly explained by the fact that the exact solution developed for anti-symmetric laminates is used to calculate buckling loads for random ply laminates [36]. Additionally, edges are considered to be free in the analytic model, but are fixed in the computational FE model, and CLPT conditions considered for the analytic solution neglect the effect of transverse shear force.

It is expected that a composite with all fibers oriented at 0 degrees will have a large critical tensile load and small transverse critical buckling load. The ply orientations for three regions in Fig. 3 are listed in Table 3 for comparison. For each region of interest, a solution is displayed for both the analytic and FE-based model. As anticipated, designs with larger uniaxial tensile loads consist primarily of 0 degree plies. While some plies are non-zero, the orientation angles reflect a design variable value one value away from a zero degree solution, as plies are allowed to change in 10 degree increments.

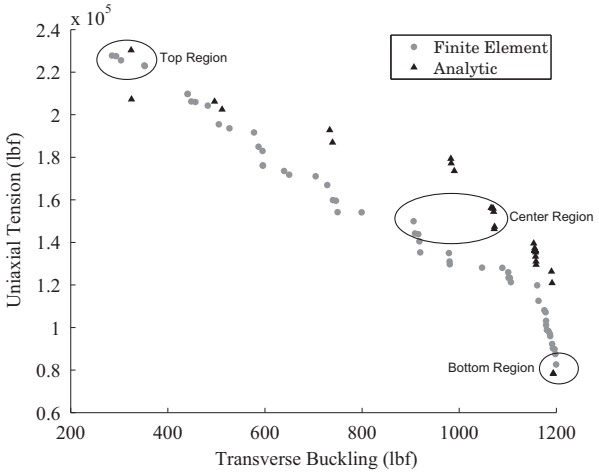

Fig. 3. Load Case 1 results: Pareto frontiers for finite element and analytic methods.

Manufactured composites are commonly symmetric and balanced. Without symmetry and balance constraints explicitly encoded, the Pareto optimal solutions shown in Table 3 mostly satisfy the balanced condition at a minimum. In nearly two-thirds of the designs, the orientation angles of each of the first four plies fell within ±10 degrees of its reflective ply.

Bending stress in a ply is directly proportional to the distance from the mid-plane. Thus bending stress distribution in the laminate is non-uniform with outer laminates subjected to higher stress as compared to inner plies. Plies located near the center of the composite do not contribute significantly to improved buckling strength. However, when considering tensile loading, the stress distribution in the laminate is uniform and thus orientation of the center plies is as important as the outer plies. Reducing the orientation angles of the inner plies is a common objective for critical buckling and tensile loads. All the solutions, independent of the region in Pareto frontier, tend to have center plies (ply 4 and 5 in Table 3) at $0° \pm 20°$. The difference in performance of all the plies arises from the difference in outer ply angles (ply 1 to ply 3 and ply 6 to ply 8 in Table 3).

When maximizing transverse critical buckling loads, a composite design solution is expected to have all fibers oriented at 90 degrees. This also leads to a small critical tensile load. Optimal designs from both models in the Bottom Region, however, do not contain plies oriented at angles larger than ±50 degrees. This result is unexpected and demonstrates the optimization challenge posed when the number of possible ply angles is increased and the design space becomes larger. Given a random initial population the genetic search is able to find solutions close to the theoretical endpoint solutions. However, the combination of computational cost, especially for the FE solution, and the definition of hypervolume convergence criteria prevent these solutions from being found in a computationally-efficient manner.

Noting that more non-dominated solutions were found when using the analytic model, and that the evaluation of the analytic model occurs at a reduced computational cost, it was hypothesized that the analytic solutions could be used as an effective seed for the FE mode. To explore this hypothesis, the Pareto optimal designs from the analytic model were evaluated in the FE model. The shift

Table 3
Load Case 1 overview: sample Pareto optimal composite designs.

Region	Analysis model	Transverse buckling (lbf)	Uniaxial tension (lbf)	Ply (deg.)							
				1	2	3	4	5	6	7	8
Top	FE	285.12	227806	0	10	0	−10	−10	0	0	10
	Analytic	324.43	230366	−10	0	10	0	0	10	0	−10
Center	FE	908.88	144204.4	−30	30	0	10	0	0	−30	30
	Analytic	1072.7	147392.8	−40	20	−10	−20	−10	0	20	−40
Bottom	FE	1199.46	82648	−40	40	40	10	−10	20	−40	40
	Analytic	1193.69	78272.4	−40	40	−20	−20	−10	30	40	−50

in objective function values for the analytic frontier when the designs are evaluated using the FE model is shown in Fig. 4(a). Due to the limitations of CLPT, when the analytic solutions are evaluated in the FE model there is a reduction in transverse buckling (average percent error of 11%) and minor changes in uniaxial tension (average percent error of 0.91%). The higher error for analytic buckling load comes from the assumptions associated with Eq. (2).

Fig. 4(b) shows the comparison of the analytic frontier evaluated using the FE model to the non-dominated solution identified when running the MOGA on the FE model. There is strong comparison amongst most of the frontier, indicating that both models converge to similar ply angle solutions. More importantly, this result supports the hypothesis that analytic solutions can be used to inform the solution of the non-dominated set when an FE model is used. Non-dominated analytic solutions can be found at a greatly reduced computational expense, and these solutions can then be evaluated in the FE model and used to seed the MOGA population for the remainder of the search.

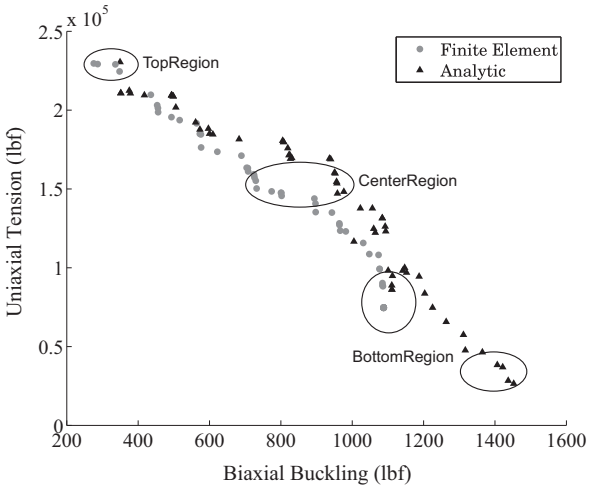

Fig. 5. Load Case 2 results: Pareto frontiers for finite element and analytic methods.

4.2. Load Case 2: uniaxial tension and biaxial buckling

To further explore the similarities and differences between the analytic and the FE model a second load case of uniaxial tension and biaxial buckling is evaluated. The buckling load is 10% of the load in the transverse direction. Fig. 5 depicts the Pareto frontiers generated by the FE and analytic method.

For large critical uniaxial tensile loads (the Top Region) the Pareto frontiers obtained from both models overlap. However, as the critical biaxial buckling load increases, the analytic model overpredicts the load. The analytic frontier predicts critical biaxial buckling loads 400 lbf greater (38%) than the largest critical biaxial buckling load generated by the FE model. Conversely, the FE model predicts larger (nearly 3000 lbf greater, or 1.3%) critical uniaxial tensile loads. This larger prediction is due to the shear additional stresses induced by the coupling terms that are better captured by FE models, resulting in smaller critical load values than the analytic model.

The design solutions corresponding to a single solution from the Top, Center, and Bottom regions of each model are reported in Table 4. As seen in the previous study, designs with the highest critical uniaxial tensile load have plies with orientations close, or equal, to zero degrees. Again, the solutions from either model do not contain ply solutions with orientation angles larger or smaller than ±50 degrees, even when biaxial buckling is maximized. There

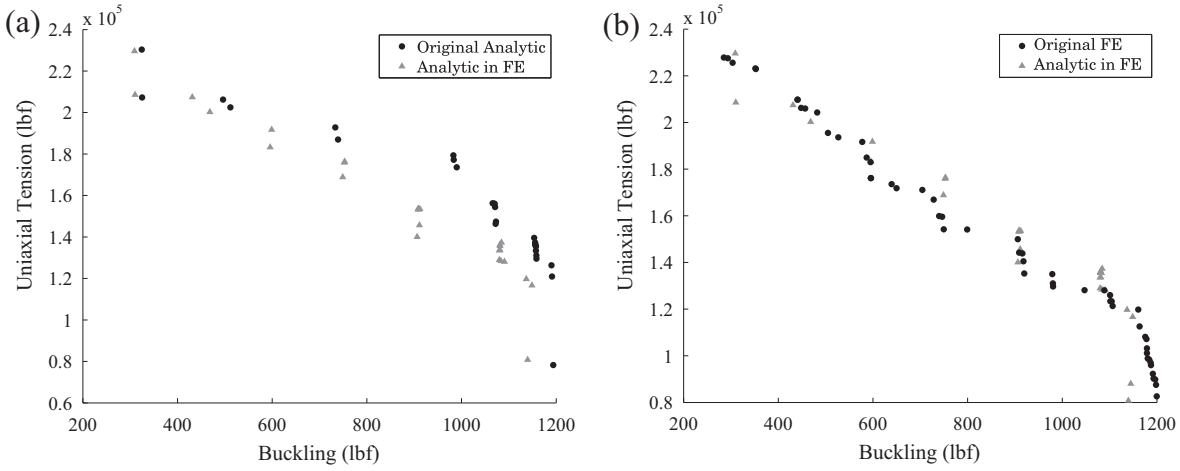

Fig. 4. (a) Cross evaluation in Load Case 1: evaluation of analytic Pareto frontier in FE model with analytic solution. (b) Cross evaluation in Load Case 1: evaluation of analytic Pareto frontier in FE model with FE solution.

Table 4
Load Case 2 overview: sample Pareto optimal composite designs.

Region	Analysis model	Transverse buckling (lbf)	Uniaxial tension (lbf)	Ply (deg.)							
				1	2	3	4	5	6	7	8
Top	FE	253.12	232742	0	0	0	−10	0	10	0	0
	Analytic	349.48	230498.3	−10	10	10	−10	−10	10	10	−10
Center	FE	726.06	157120.6	−30	20	10	−10	−10	0	−30	20
	Analytic	826.79	169225.3	−30	10	−10	0	−10	10	10	−40
Bottom	FE	1088.12	74654.6	−40	40	40	0	−10	30	−40	40
	Analytic	1452.47	26488.9	40	50	50	50	−40	50	−40	50

is symmetry, but to a lesser extent than those displayed in Table 3, and balanced designs are not present. Comparing only the analytic designs of Load Case 1 and Load Case 2, the Pareto optimal Load Case 1 designs follow a symmetric pattern to a greater extent than those of Load Case 2.

As discussed previously, the limitations of CLPT yield an analytic model known to over-predict buckling loads [36]. However, when compared with the first load case of transverse buckling, the over prediction associated with biaxial buckling appears much larger, as shown in Fig. 6. Fig. 6(a) shows how, when the analytic model solution are cross-evaluated in the FE model, the predicted buckling and tension loads are reduced. The average biaxial buckling error between the analytic result and the same design evaluated in the FE model is 14.1% with a standard deviation of 16%. For uniaxial tension, the average error is 4.95% and the standard deviation 7%. These average standard errors are larger than the errors associated with the first load case considered. This can be attributed to a much smaller percentage of balanced laminates, further diverging from the assumptions of Eq. (2).

While the designs may see greater average error when cross-evaluated, a useful outcome is that designs with the largest critical buckling load in the analytic solution have the largest critical buckling load in the FE model. This is important because rank reversals of buckling loads would suggest more significant theoretical limitations of the analytic model than over-predicting performance. A similar outcome was found for the uniaxial tensile load.

Building on the discussion from the first loading case studied, the results presented in Fig. 6(b) compare the analytic solutions after being evaluated in the FE model with the solutions obtained from the MOGA when using the FE model. While the analytic model may over-predict the performance of the composite solutions for buckling (the best solution withstands approximately 1400 lbf), these solutions dominate the solutions found when optimizing with the FE model. Elsewhere in the space there is useful similarity between predicted performances, except in the regions where the buckling load is between 700 and 1000 lbf. Despite the differences in this region of the performance space, the MOGA using the analytic model identified solutions that would be non-dominated with respect to the solutions generated using the FE model. These results further support the hypothesis that an analytic solution can be used as an effective starting point for a MOGA using the FE model, regardless of what load scenario is being considered.

4.3. Comparing the analytic solutions for Load Case 1 and Load Case 2

If analytic solutions are to be used as an effective seeding strategy, they offer greater value to the optimization algorithm if they are robust to load scenario definition. Fig. 7 shows the results of cross-evaluating the analytic model solutions across load cases. As uniaxial tension is considered in both load cases, the values for this axis remain constant.

When the results from Load Case 1 are evaluated under biaxial buckling, there is a reduction in critical buckling load. A similar, but opposite trend is observed when Pareto optimal designs produced for biaxial buckling load are cross-evaluated under transverse buckling. The largest percent difference in buckling load occurs in the middle of the frontier, rather than at the endpoints. Despite these differences, the two results can largely be used interchangeably with minimal variation in predicted performance.

4.4. Load Case 3: uniaxial tension and biaxial buckling with out-of-plane pressure

Previous work has demonstrated that computational run-time can be reduced and solution quality can be improved when a more

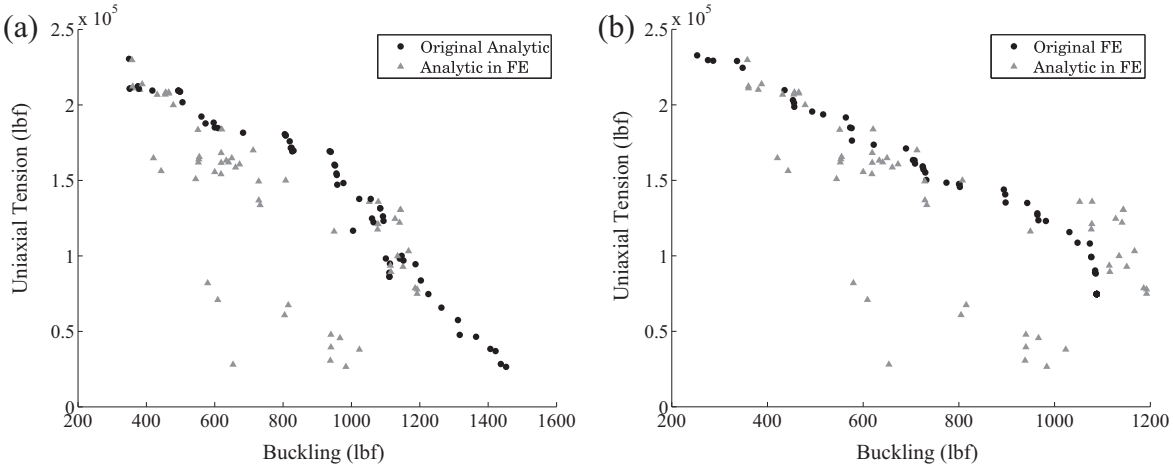

Fig. 6. (a) Cross evaluation in Load Case 2: evaluation of analytic Pareto frontier in FE model with analytic solution. (b) Cross evaluation in Load Case 2: evaluation of analytic Pareto frontier in FE model with FE solutions.

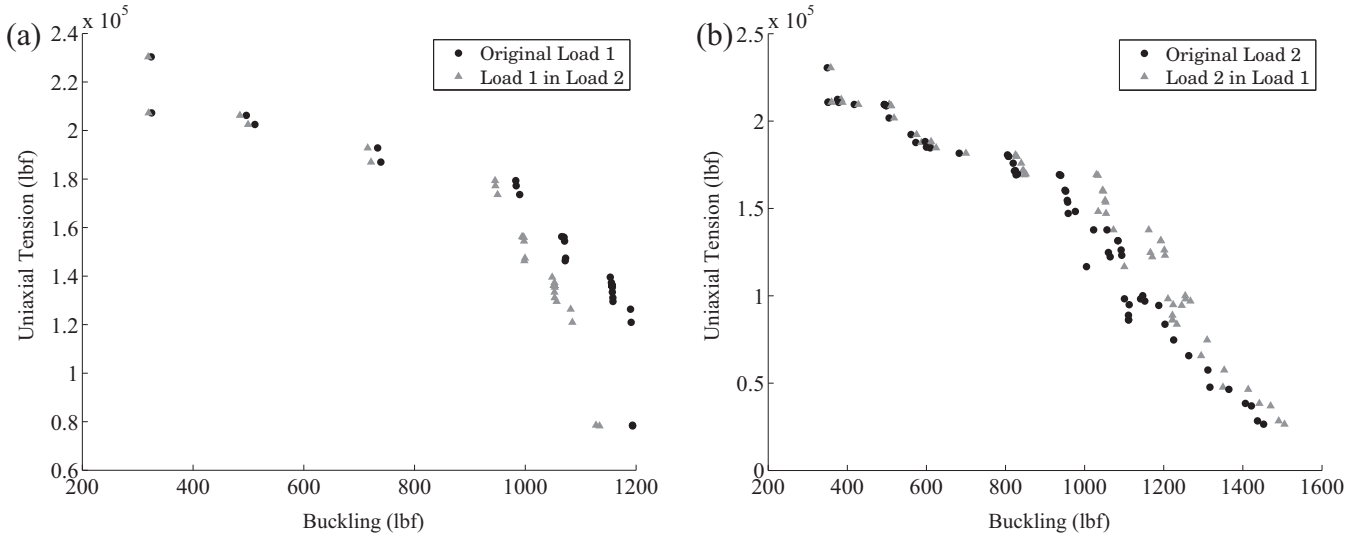

Fig. 7. (a) Cross evaluation across the Load Cases: analytic Load Case 1 cross evaluated in analytic Load Case 2. (b) Cross evaluation across the load cases: analytic Load Case 2 cross evaluated in analytic Load Case 1.

effective initial population is provided [37]. The results introduced in the previous sections highlight the potential for solutions from the analytic model to serve as a surrogate initial population for the FE model. The limitations associated with some of the CLPT formulations do not hinder the analysis of composites with large uniaxial tensile loads. However, when analyzing designs with larger buckling loads, the analytic model suffers from lower accuracy and tends to over predict the critical buckling load. With these conclusions in mind, a more realistic load case is implemented in this section in which biaxial buckling with out-of-plane pressure and uniaxial tension are considered.

When considering an aircraft fuselage, a pressure differential exists because the inside of the fuselage is pressurized at atmospheric pressure and the outside pressure is comparably very low. This out-of-plane differential pressure acts on a small section of the fuselage. When developing the model for analysis, a two-step loading process is used where the composite is first subjected to the out-of-plane pressure and then to biaxial compression. Due to the relatively high pressure and thinness of the laminate, deflection is very large and conventional CLPT assumptions are not valid.

A valid and accurate analytic model is extremely difficult to develop for such a two-step loading process. As a result, only a computational FE model is able to determine the critical loads for uniaxial tension and biaxial buckling with out-of-plane pressure. Typical differential pressures acting on a fuselage during flight vary from 11 to 13 psi.

The most common laminate used in fuselage construction is a 16 ply laminate with a single ply thickness of 0.01 in. [2]. However, increasing the number of plies increases the number of design variables considered and the computational cost of the optimization. It is expected that the ply orientation trends in terms of Pareto frontier location remain consistent for multilayered laminates. Therefore, an 8 ply laminate is considered and the pressure is scaled to avoid large displacements. A constant uniform pressure of 1.4 psi is assumed.

As no reliable analytic model for biaxial buckling with out-of-plane pressure exists, Fig. 8 depicts the set of non-dominated Pareto solutions associated with the FE model. The presence of out-of-plane pressure increases the critical buckling load of the composite, which is counterintuitive to the general notion that an increase in loading decreases material strength. This is a generic phenomenon applicable to thin structures subjected to

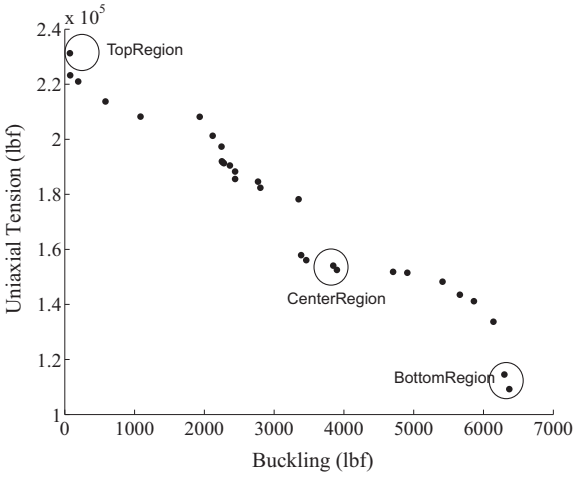

Fig. 8. Load Case 3 results: finite element Pareto frontier.

out-of-plane pressure and axial compression, and was reported experimentally by Lo et al. [38]. This behavior was also studied using FE methods for composite cylinders with cutouts by Tafreshi [39] and Hilburger [40]. The strengthening effect is a result of the out-of-plane pressure reducing the initial geometric non-linearity, which increases the critical buckling load. However, at higher pressures the deformation goes beyond repairing the non-linearity and causes the critical buckling load to decrease.

Generating the frontier presented in Fig. 8 required 5821 function evaluations. An initial set of random solutions was used as a starting population and the algorithm converged after 38 generations. When developing an optimal composite, designers may not have the time to allow a MOGA to complete the number of function evaluations required to produce a set of Pareto optimal designs. This is a greater concern as the set of allowed ply orientation angles increases. For example, an 8 ply composite with a set of 10 allowable angles yields a design space consisting of 1E + 08 combinations. If the set of allowable angles is increased to 20, the design space is increased by a factor of 256, yielding 2.56E + 10 possible combinations.

A design configuration associated with the Top, Center, and Bottom Regions of Fig. 8 are represented in Table 5. Unlike the

Table 5
Load Case 3 overview: sample Pareto optimal composite designs.

Analysis	Region	Buckling with pressure (lbf)	Uniaxial tension (lbf)	Ply (deg.)							
				1	2	3	4	5	6	7	8
Finite element	Top	73.998	231256	0	0	10	−10	0	0	0	0
	Center	3847.4	154086	−20	10	50	0	10	10	−20	30
	Bottom	6298.8	114529	−20	0	60	10	20	10	−30	70

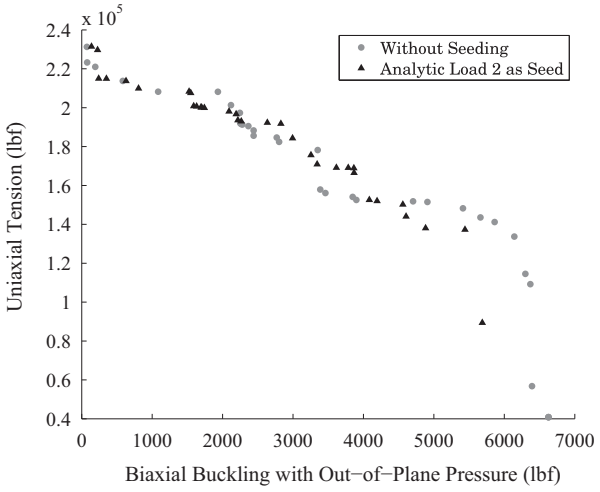

Fig. 9. Effect of seeding: analytic solution used as seed in Load Case 3.

previous load cases, the design with the smallest critical uniaxial tensile load has ply orientation angles as large as 70°. The smallest biaxial buckling with pressure design is comprised of plies with 0° orientation angles, except for two inner plies. In comparison with previous load cases, solutions to Load Case 3 barely show degrees of balance and ply symmetry. From a buckling perspective, the lowest buckling force is tolerated by a composite with ply orientations of 0 degrees, while the highest buckling force is achieved by ply orientation angles of ±45 degrees. For Load Case 3 the highest buckling performance is achieved by 0°/90° plies, producing design configurations different from those of Load Case 1 and Load Case 2. This difference is significant when increasing critical buckling loads only. In terms of critical tensile loads, all three load cases show very similar strengths as reported in Table 3–5.

When a designer has limited information about the nature of the solution space, there are advantages to using a random initial population in a genetic search. However, a more informed set of initial solutions can reduce the computational expense of the optimization and lead to improved solution quality. To demonstrate this, the design configurations obtained from the analytic Pareto frontier associated with Load Case 2 is used as the initial population for Load Case 3. Recall that no analytical solution could be obtained for Load Case 3, and Load Case 2 and 3 represent a more common loading scenario.

The computational time associated with producing the analytic Pareto frontier for Load Case 2 was less than 90 min. The non-dominated points from the analytic biaxial buckling and uniaxial tension frontier were then used as the initial seed for the FE Load Case 3 model. The total runtime of the simulation was 20 h on a 4-core parallel processing cluster. To generate the Pareto frontier shown in Fig. 9, 1,409 functional evaluations were required. This is a nearly 80% reduction in computational run-time. From a solution quality perspective, the small differences between the two frontiers are attributed to the stochastic nature of a MOGA. Thus, Fig. 9 supports the hypothesis of using analytic solutions as a seed solution, even when the loading conditions change.

5. Discussion

In addition to exploring whether analytic models could be used as an effective seed for a FE model, a secondary objective of this work was to explore the regions of the performance space populated by different analysis models while considering multiple loading scenarios. Creating analytical solutions for these problems often require assumptions or simplifications to be made to achieve closed form solutions. Yet, these assumptions and simplifications often reduce the accuracy of the prediction. This is evident in the critical buckling load analysis, as the analytical solution for a fully coupled composite plate (populated B and D matrix) does not exist. The optimization results demonstrated that for the loading cases considered, the buckling solutions were drastically different for the two different models. Additionally, Load Case 3 introduced a realistic loading scenario for an aircraft fuselage panel where an analytic solution was not available. Because the deflection of the panel is relatively large, conventional CLPT assumptions do not hold.

Composite components also see multiple loading conditions while in service. This introduces challenges from a design problem formulation perspective, and the optimal design for one loading scenario may not satisfy the requirements for another. Based on critical buckling and tensile load values reported in the previous sections, solutions from Load Case 1 and 2 were found to be interchangeable. This result is further supported by Figs. 10 and 11, which show that the optimum orientations for Load Case 1 and Load Case 2 are almost identical. Figs. 10–12 depict parallel coordinate plots of the Pareto optimal designs for the FE model for Load Case 1, Load Case 2 and Load Case 3, respectively.

The designs depicted in Figs. 10 and 11 appear to follow a symmetric and balanced pattern. This behavior is not apparent in Fig. 12. The addition of pressure results in balanced and symmetric laminates at lower buckling loads. To achieve high critical buckling loads, ply orientations are not balanced or symmetric so that the buckling of the panel can be counteracted. Therefore designs for Load Case 3 require a different laminate configuration compared to the first two loading cases.

The solutions to the three load cases also demonstrate that performance may be better achieved when a finer granularity of orientation angles are considered. Much of the current literature limits the possible orientation angles to a very small subset. This limitation may reduce manufacturing complexity but can also artificially constrain system performance. As the design space becomes larger when more angle possibilities are considered, so will the computational cost associated with solving the optimization problem. In this work, running a MOGA with orientation angles considered at 10 degree intervals and a random initial population took 4 days to produce a solution when using a computational FE model.

When an analytical model could be formulated, the process of finding solutions was 50–60 times faster than the process for finding solutions using a computational FE model. This outcome is significant because the results presented in the previous section demonstrate that analytical solutions are a more effective starting population than randomly generated initial designs. The computational savings achieved by seeding the initial population with these

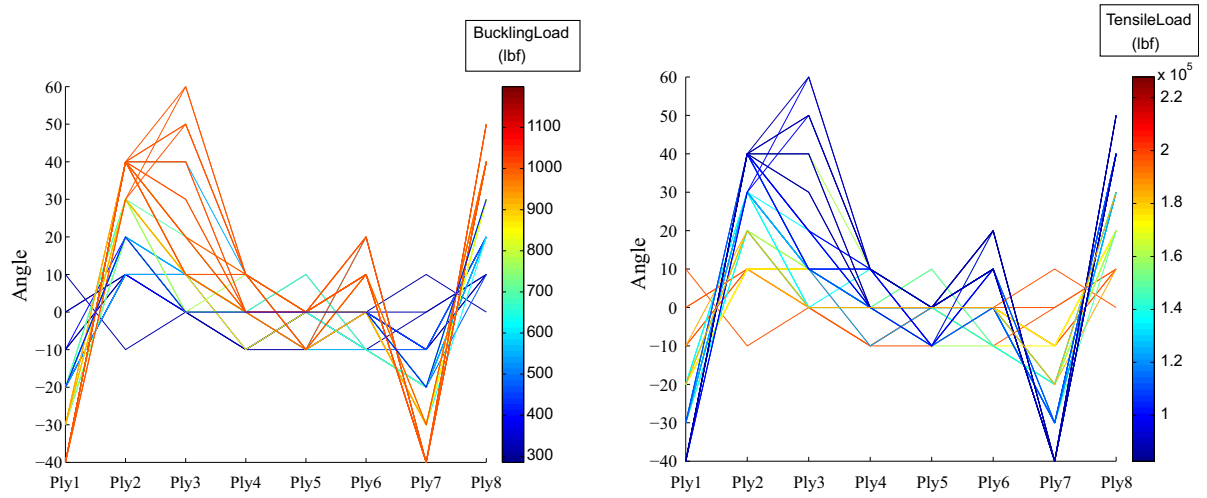

Fig. 10. Parallel coordinates plot for Load Case 1: influence of ply angles of Pareto frontier on the response of laminate.

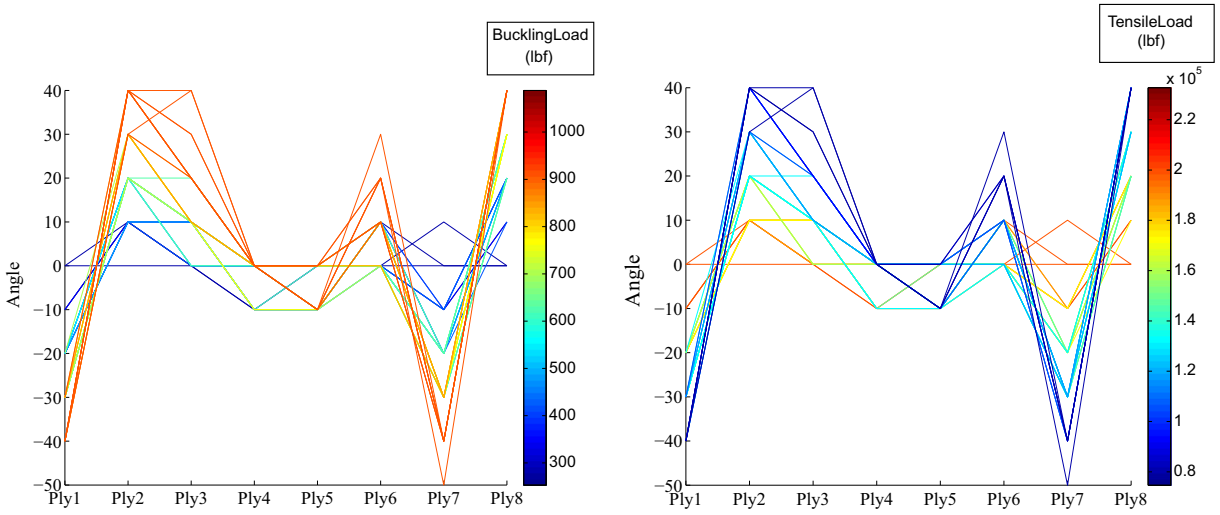

Fig. 11. Parallel coordinates plot for Load Case 2: influence of ply angles of Pareto frontier on the response of laminate.

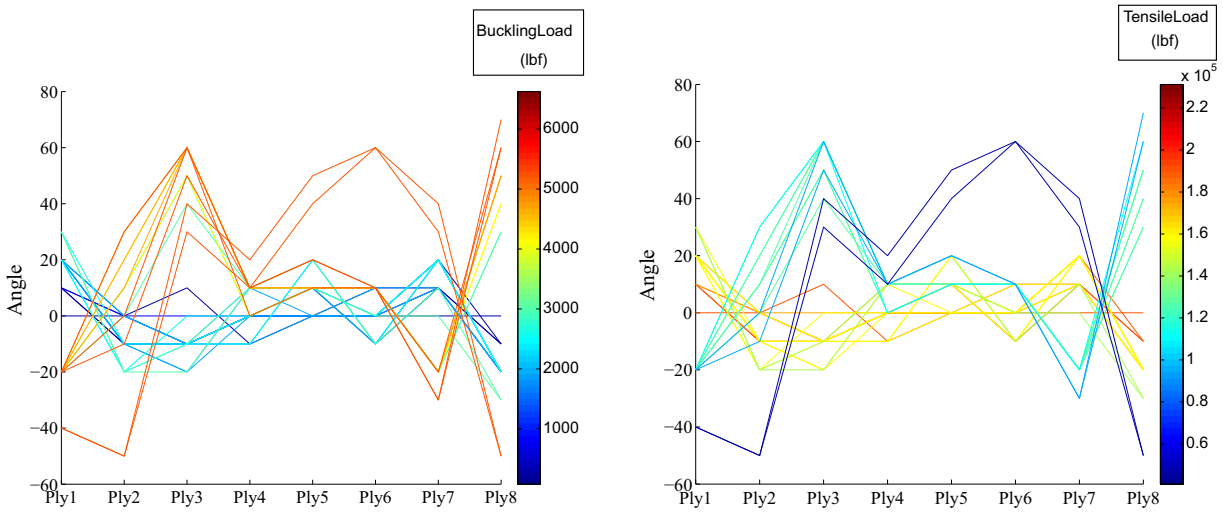

Fig. 12. Parallel coordinates plot for Load Case 3: influence of ply angles of Pareto frontier on the response of laminate.

analytical solutions will allow more complex composite optimization problems to be considered in future work. Further, using these solutions provided benefits even when the analytical model did not present a complete match to the loading scenario actually encountered by the composite. Seeding the algorithm with a solution for a similar analytic problem yielded a solution in less than one day, an 80% decrease in computational time.

6. Conclusion and future work

Analytical models can often be overlooked because of the simplifications required to arrive at a viable closed-form solution. Also, it is not possible to model all complex loading scenarios with a closed-form analytical model. In this work, a multi-objective genetic algorithm was implemented to optimize the performance of an 8-ply composite laminate for three different load cases. The design variables corresponded to the ply orientation angles, whose acceptable values were defined by a set of angles ranged between ±90 degrees in 10 degree intervals. Two different modeling approaches, analytic and computational FE models, were used to solve for the critical load values.

The simulations run in this work demonstrate the continued usefulness of analytic models, particularly in an optimization context. For a subset of loading scenarios and performance objectives the predicted performance of the composite had only slight differences when comparing the outcomes of analytical and FE models. As the problem expanded to multiple load cases, the optimum solution was found to be different, but simplified load case solutions did show some overlap with solutions from more complex loading cases. In loading scenarios where results match closely between the analytical and FE model, significant reductions in computational cost can be achieved using the analytical model.

More importantly, this paper demonstrates that while complex loading cases will have a unique set of solutions, using results from simplified loading scenarios as a seed can lead to reduced computational cost and improved solution quality. Using simplified model solution sets as a seed led to a reduction in run-time of 80% for some of the studies in this work. Additionally, regions of the solution space where configurations are identical between loading cases can be used to identify composite panel solutions that have a greater level of robustness to changes in loading while the composite is in service. This is important for parts that are expected to see a wide variety of loads.

As increased computational power becomes more ubiquitous it is less burdensome to use complex computational FE models. Yet, it is likely that the design space of future composite design problems will be significantly larger than the one considered in this paper. As optimization problems are formulated around composites consisting of a larger number of plies and acceptable orientation angles, the difficulty of effectively searching such a space can increase exponentially. Future work in this area could explore how knowledge about composite panel design problems could be further leveraged to decrease the computational cost associated with optimization. While it may be necessary to use FE models for complex loading scenarios, different constraints on the orientation angles of the plies could reduce the size of the design space that must be explored.

With the exception of biaxial buckling with out-of-plane pressure the non-dominated solutions found in this work followed a symmetric and balanced pattern. Enforcing a symmetric and/or balanced constraint on feasible designs could reduce computational run times and reinforce the current manufacturing practices associated with composite design. Other work could explore if a basic set of simplified loading cases could be identified to serve as effective seeds for more complicated loading scenarios.

Acknowledgements

We gratefully acknowledge support from the National Science Foundation through NSF CAREER Grant No. CMMI-1054208. Any opinions, findings, and conclusions presented in this paper are those of the authors and do not necessarily reflect the views of the National Science Foundation.

References

[1] Sun M, Hyer MW. Use of material tailoring to improve buckling capacity of elliptical composite cylinders. AIAA J 2008;46(3):770–82.
[2] Jegley DC, Tatting BF, Gurdal Z. Optimization of elastically tailored tow-placed plates with holes. In: 44th AIAA/ASME/ASCE/AHS structures, structural dynamics and materials conference. Norfolk; 2003.
[3] Ghiasi H, Pasini D, Lessard L. Optimum stacking sequence design of composite materials Part I: constant stiffness design. Compos Struct 2009;90(1):1–11.
[4] Johansen L, Lund E, Kleist J. Failure optimization of geometrically linear/nonlinear laminated composite structures using a two-step hierarchical model adaptivity. Comput Methods Appl Mech Eng 2009;198(30–32):2421–38.
[5] Georgopoulou C, Ciannakoglou K. A multi-objective metamodel-assisted memetic algorithm with strength-based local refinement. Eng Optim 2009;41(10):909–23.
[6] Rocha I, Parente E, Melo A. A hybrid shared/distributed memory parallel genetic algorithm for optimization of laminate composites. Compos Struct 2014;107:288–97.
[7] Ferreira R, Rodrigues H, Guedes J. Hierarchical optimization of laminated fiber reinforced composites. Compos Struct 2014;107:246–59.
[8] Walker M, Smith R. A technique for the multiobjective optimisation of laminated composite structures using genetic algorithms and finite element analysis. Compos Struct 2003;62(1):123–8.
[9] Irisarri F-X, Bassir DH, Carrere N, Maire J-F. Multiobjective stacking sequence optimization for laminated composite structures. Elsevier 2009;69:983–90.
[10] Adali S, Walker M, Verijenko V. Multiobjective optimization of laminated plates for maximum prebuckling, buckling and postbuckling strength using continuous and discrete ply angles. Compos Struct 1996;35:117–30.
[11] Walker M, Reiss T, Adali S. Multiobjective design of laminated cylindrical shells for maximum torsional and axial buckling loads. Comput Struct 1997;62(2):237–42.
[12] Alhajahmad A, Abdalla MM, Gurdal Z. Optimal design of tow-placed fuselage panels for maximum strength with buckling considerations. J Aircr 2010;47(3):775–82.
[13] Irisarri F-X, Laurin F, Leroy F-H, Maire J-F. Computational strategy for multiobjective optimization of composite stiffened panels. Compos Struct 2011;93:1158–67.
[14] Lee D, Morillo C, Bugeda G, Oller S, Onate E. Multilayered composite structure design optimisation using distributed/parallel multi-objective evolutionary algorithms. Compos Struct 2012;94(3):1087–96.
[15] Topal U. Multiobjective optimum design of laminated composite annular sector plates. Steel Compos Struct 2013;14(2):121–32.
[16] Almeida F, Awruch A. Design optimization of composite laminated structures using genetic algorithms and finite element analysis. Compos Struct 2009;88(3):443–54.
[17] Panesar A, Weaver P. Optimisation of blended bistable laminates for a morphing flap. Compos Struct 2012;94(10):3092–105.
[18] Van Campen J, Kassapoglou C, Gurdal Z. Generating realistic laminate fiber angle distributions for optimal variable stiffness laminates. Compos Part B: Eng 2012;43(2):354–60.
[19] Lansing W, Dwyer W, Emerton R. Application of fully stressed design procedures to wing and empennage structures. J Aircr 1971;8(9):683–8.
[20] Jibawy A, Desmorat B, Vincenti A. Structural rigidity optimization of thin laminated shells. Compos Struct 2013;95:35–43.
[21] Ghiasi H, Pasini D, Lessard L. Layer separation for optimization of composite laminates. In: ASME 2008 international design engineering technical conferences and computers and information in engineering conference. New York; 2008.
[22] Hirano Y. Optimum design of laminated plates under axial compression. AIAA J 1979;17(9):1017–9.
[23] Walker M, Reiss T, Adali S, Weaver P. Application of MATHEMATICA to the optimal design of composite shells for improved buckling strength. Eng Comput 1998;15(2):260–7.
[24] Waddoups M. Structural airframe application of advanced composite materials-analytical methods. Air Force Materials Library, Wright-Patterson Air Force Base; 1969.
[25] Verette R. Stiffness, strength and stability optimization of laminated composites. Hawthorne: Northrop Aircraft Co.; 1970.
[26] Weaver P. Designing composite structures: lay-up selection. J Aerosp Eng 2002;216:105–16.
[27] Park W. An optimal design of simple symmetric laminates under the first ply failure criterion. J Compos Mater 1982;16(4):341–55.
[28] Cairo R. Optimum design of boron epoxy laminates. Bethpage: Grumman Aircraft Engineering Corporation; 1970.

[29] Soremekun G. Genetic algorithm for composite laminate design and optimization; 1997.
[30] ABAQUS Version 6.12, Providence, RI: Dassault Systems Simulia Corp; 2012.
[31] Whitney J. Structural analysis of laminated anisotropic plates. Lancaster, Pa: Technomic Pub. Co.; 1987.
[32] Jones R. Mechanics of composite materials. Philadelphia, PA: Taylor & Francis; 1999.
[33] Deb K. A fast and elitist multiobjective genetic algorithm: NSGA-II. IEEE Trans Evol Comput 2002;6(2):182–97.
[34] Henderson J. Laminated plate design using genetic algorithms and parallel processing. Comput Syst Eng 1994;5(4–6):441–53.
[35] Kere P, Lento J. Design optimization of laminated composite structures using distributed grid resources. Compos Struct 2005;71(3–4):435–8.
[36] Kant T, Swaminathan K. Analytic solutions for free vibration of laminated composite and sandwich plates based on a higher-order refined theory. Compos Struct 2001;53(1):73–85.
[37] Foster G, Ferguson S, Donndelinger J. Creating targeted initial populations for genetic product searches in heterogeneous markets. Eng Optim 2014;46(12):1729–47.
[38] Lo H, Crate H, Schwartz B. Buckling of thin walled cylinder under axial compression and internal pressure. National Advisory Committee for Aeronautics, Langley Field; 1949.
[39] Tafreshi A. Buckling and post-buckling analysis of composite cylindrical shells with cutouts subjected to internal pressure and axial compression loads. Int J Press Vessels Pip 2002;79(5):351–9.
[40] Hilburger M, Waas A, Starnes J. Response of composite shells with cutouts to internal pressure and compression loads. AIAA J 1999;37(2):232–7.